*Inorg. Chem.* **2007**, *46*, 7178–7188

# A Dinuclear Copper(II) Complex with Adeninate Bridge Ligands and Prominent DNA Cleavage Activity. Structural and Spectroscopic Characterization and Magnetic Properties

**José Luis García-Giménez,[†] Gloria Alzuet,[†] Marta González-Álvarez,[†] Alfonso Castiñeiras,[‡] Malva Liu-González,[§] and Joaquín Borrás*,[†]**

*Departament de Química Inorgànica. Facultat de Farmàcia. Universitat de València. 46100- Burjassot, Spain, Departamento de Química Inorgánica. Facultad de Farmacia. Universidad de Santiago de Compostela. 15703- Santiago de Compostela, Spain, and SCSIE, Universitat de València. 46100- Burjassot, Spain*

Received April 20, 2007

A new dinuclear copper(II) complex has been synthesized and structurally characterized: $[Cu(\mu\text{-ade})(tolSO_3)(phen)]_2 \cdot 2H_2O$ (Hade = adenine, $tolSO_3^-$ = toluenesulfonate anion). Its magnetic properties and electronic paramagnetic resonance (EPR) spectra have been studied in detail. The compound has two metal centers bridged by two adeninate NCN groups. The coordination geometry of the copper(II) ions in the dinuclear entity is distorted square pyramidal, with the four equatorial positions occupied by two phenanthroline N atoms and two N atoms from different adenine molecules. The axial position is occupied by one sulfonate O atom. Magnetic susceptibility data show antiferromagnetic behavior with an estimated exchange constant of $-2J = 65$ cm$^{-1}$. The EPR spectrum has been obtained at both X- and Q-band frequencies; a study at different temperatures has been carried out at the latter. Above 20 K, the Q-band spectra are characteristic of $S = 1$ species with a small zero-field splitting parameter ($D = 0.0970$ cm$^{-1}$). A detailed study of the DNA–complex interaction has been performed. The title complex efficiently cleaves the pUC18 plasmid in the presence of reducing agents. Both the kinetics and the mechanism of the cleavage reaction are examined and described herein.

## Introduction

The interaction of nucleic acids and their constituents with metal ions has been the subject of extensive study because of the chemical and biological potential of these compounds.[1] Much of the available information obtained to date stems from knowledge about the structure and reactivity of artificial, biomimetic systems based on transition-metal complexes containing nucleobase ligands or analogs.[2] Only a few copper(II) structures with adenine have been reported, including anionic adeninato ($ade^-$),[3−7] neutral adenine (Hade),[5,8−11] and cationic adeninium ($H_2ade^+$).[12−14] In these compounds, the different adenine species link to copper(II)

* To whom correspondence should be addressed. E-mail: Joaquin.Borras@uv.es. Fax: 34-963544960.

[†] Departament de Química Inorgànica. Facultat de Farmàcia. Universitat de València.

[‡] Departamento de Química Inorgánica. Facultad de Farmacia. Universidad de Santiago de Compostela.

[§] SCSIE, Universitat de València.

(1) Bugella-Atamirano, E.; Choquesillo-Lazarte, D.; González-Pérez, J. M.; Sánchez-Moreno, M. J.; Marín-Sánchez, R.; Martín-Ramos, J. D.; Covelo, B.; Carballo, R.; Castiñeiras, A.; Niclós-Gutiérrez, J. *Inorg. Chim. Acta*. **2002**, *339*, 160−170.

(2) Lippert, B. *Coord. Chem. Rev.* **2000**, *200*−*202*, 487−516.

(3) Marzotto, A.; Ciccarese, D.; Clemente, A.; Valle, G. *J. Chem. Soc., Dalton Trans*. **1995**, 1461−1468.

(4) Sakaguchi, H.; Anzai, H.; Furuhata, K.; Ogura, H.; Iitaka, Y.; Fujita, T.; Sakaguchi, T. *Chem. Pharm. Bull.* **1978**, *26*, 2465−2474.

(5) Sletten, E. *Acta Crystallogr*. **1969**, *B25*, 1480−1491.

(6) González-Pérez, J. M.; Alarcón-Payer, C.; Castiñeiras, A.; Pivetta, T.; Lezama, L.; Choquesillo-Lasarte, D.; Crisponi, G.; Niclós-Guitérrez, J. *Inorg. Chem.* **2006**, *45*, 877−882.

(7) García-Terán, J. P.; Castillo, O.; Luque, A.; García-Couceiro, U.; Román, P.; Lezama, L. *Inorg. Chem.* **2004**, *43*, 4549−4551.

(8) Terzis, A.; Beauchamp, A. L.; Rivest, R. *Inorg. Chem.* **1973**, *12*, 1166−1170.

(9) de Meester, P.; Skapski, A. C. *J. Chem. Soc., A* **1971**, 2167−2169.

(10) Tomita, K.; Izuno, T.; Fujiwara, T. *Biochem. Biophys. Res. Commun*. **1973**, 96−99.

(11) Rojas-González, P. X.; Castiñeiras, A.; González-Pérez, J. M.; Choquesillo-Lasarte, D.; Niclós-Guitérrez, J. *Inorg. Chem.* **2002**, *41*, 6190−6192.

(12) de Meester, P.; Skapski, A. C. *J. Chem. Soc., Dalton Trans*. **1972**, 2400−2404.

(13) de Meester, P.; Skapski, A. C. *J. Chem. Soc., Dalton Trans*. **1973**, 424−427.

(14) Brown, D. B.; Hall, J. W.; Helis, H. M.; Walton, E. G.; Hodgson, D. J.; Hatfield, W. E. *Inorg. Chem*. **1977**, *16*, 2675−2680.



10.1021/ic700751j CCC: $37.00 
Published on Web 07/13/2007

either through the N(9) donor atom or through the N(3),N(9), the N(7),N(9), or the N(3),N(7),N(9) in a $\mu$-bridging mode. Chemically, the NCN groups of the adenine ligand offer the possibility of forming a bridge between the two copper centers as one of many coordination mode possibilities. Biologically, these compounds represent a new and interesting group of metal complexes with nuclease activity.

In recent years, there has been substantial interest in the rational design of novel transition-metal complexes that bind and cleave duplex DNA with high sequential or structural selectivity.[15−17] In this context, polynuclear copper(II) compounds have gained prominence ever since Karlin and coworkers[18−19] showed that nuclearity is a crucial parameter in oxidative cleavage, with the synergy between the two metal ions contributing to high nucleolytic efficiency. Our recent results concerning the nuclease activity of several mononuclear and dinuclear copper(II) complexes with *N*-sulfonamidate derivatives corroborate and confirm Karlin's findings.[20,21]

Oxidative DNA damage is perhaps one of the most crucial events in the cytotoxicity of reactive oxygen species (ROS). DNA lesions resulting from exposure to ROS include modified bases, abasic sites, single- and double-strand breaks, and DNA−protein cross-links.[22−24] Furthermore, ROS can act as secondary messengers in intracellular signaling cascades and can even produce cellular signaling cascades that induce cell senescence and apoptosis.[25,26]

In addition to the biological relevance of transition-metal complexes containing more than one metal atom per molecule, dinuclear copper(II) complexes have been used extensively to derive magnetostructural correlations, which, in turn, allow for a better understanding of the nature of the spin−spin coupling phenomena in different structural arrangements. Furthermore, these compounds have proven to be useful precursors in the syntheses of high-nuclearity clusters with novel supramolecular features.[27−30]


(15) Geierstanger, B. H.; Marksich, M.; Dervan, P. B.; Wemmer, D. E. *Science.* **1994**, *266*, 646−650.
(16) Liu, C.; Zhou, J.; Li, Q.; Wang, L.; Liao, Z.; Xu, H. *J. Inorg. Biochem.* **1996**, *75*, 233−240.
(17) Patviel, G.; Bernadou, J.; Meunier, B. *Angew. Chem., Int. Ed. Engl.* **1995**, *34*, 746−769.
(18) Humpreys, K. J.; Hohnson, A. J.; Karlin, K. D.; Rokita, S. E. *J. Biol. Inorg. Chem*. **2002**, *7*, 835−842.
(19) Li, L.; Karlin, K. D.; Rokita, S. E. *J. Am. Chem. Soc*. **2005**, *127* (2), 520−521.
(20) González-Álvarez, M.; Alzuet, G.; Borrás, J.; Pitié, M.; Meunier, B. *J. Biol. Inorg. Chem*. **2003**, *8*, 644−652.
(21) Cejudo, R.; Alzuet, G.; González-Álvarez, M.; García-Gimenez, J. L.; Borrás, J.; Liu-González, M. *J. Inorg. Biochem.* **2006**, *100*, 70−79.
(22) Halliwell, B.; Aruoma, O. I. *FEBS Lett.* **1991**, *281*, 9−19.
(23) Dizdaroglu, M. *Free Radical Biol. Med*. **1991**, *10*, 225−242.
(24) Dizdaroglu, M. *Mutat. Res*. **1992**, *275*, 331−342.
(25) Valko, M.; Rhodes, C. J.; Moncol, J.; Izakovic, M.; Mazur, M. *Chem.-Biol. Interact*. **2006**, *160*, 1−40.
(26) Valko, M.; Leibfritz, K.; Moncol, J.; Cronin, M. T. D.; Mazur, M.; Telser, J. *Int. J. Biochem. Cell Biol*. **2007**, *39*, 44−84.
(27) Winpenny, R. *Adv. Inorg. Chem*. **2001**, *52*, 1−111.
(28) Kahn, O. *Molecular Magnetism*; VCH: Weinheim, Germany, 1993.
(29) Mukherjee, A.; Rudra, I.; Naik, S. G.; Ramesasha, S.; Nethaji, M.; Chakravarty, A. R. *Inorg. Chem*. **2003**, *42*, 5660−5668.
(30) Gram, B.; Siccia, L.; Fallon, G. D.; Hearn, M. T. W.; Mabbs, F. E.; Moubaraki, B.; Murray, K. S. *J. Chem. Soc., Dalton Trans*. **2001**, 1216−1232.


**Chart 1**

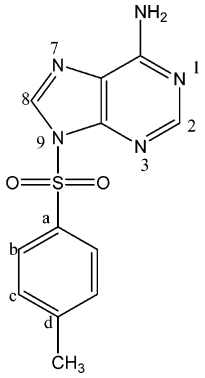


In the present article, the synthesis and crystal structure of *N*-9-(toluenesulfonyl)adenine (HL) (Chart 1) are described. The choice of this ligand was based on our previous studies that have indicated that copper(II) complexes with benzene, toluene or naphthalene sulfonyl derivatives bearing heteroaromatic rings (pyridine, thiazole, or benzothiazole) present potent nuclease activity.[20,21] The inclusion of adenine could increase this nuclease activity of the compounds. The reaction of Cu(II) with this ligand gives rise to a dinuclear copper(II) compound. The structural determination of single crystals of this complex gives the formula $[Cu(\mu\text{-ade})(tolSO_3)(phen)]_2 \cdot 2H_2O$, indicating that *N*-9-(toluenesulfonyl)-adenine is hydrolyzed in the reaction with Cu(II) to afford adeninate and toluenesulfonate anions. Because adenine is a nucleobase and $[Cu(phen)_2]^{2+}$ has an important nucleolytic effect, the presence of adeninate and phenanthroline in the coordination polyhedron of Cu(II) may lead to high nuclease activity.

The DNA−copper complex interactions have been analyzed by means of quenching the fluorescence of the DNA-EB system, DNA thermal denaturation, and viscosimetric measurements. The nuclease activity, a degradation kinetic study, and the ROS species implicated in the DNA cleavage mechanism are all reported.

## Experimental Section

**Materials and Methods.** Copper salts, other chemicals, and solvents were commercially available (Sigma) in high purity and used as received. Plasmid pUC18 (0.25 $\mu$g/$\mu$L, 750 $\mu$M in nucleotides) in TE (tris 10 mM and EDTA 1 mM, pH= 8.0) was purchased from Roche Diagnostics, Germany. CT DNA (type XV) was obtained from Sigma. Solutions of the metal complexes and other reagents for strand scission experiments were prepared fresh daily. Elemental analyses were performed with a CE Instrument EA 1110 CHNS analyzer. Infrared spectra were recorded on a Mattson Satellite FTIR spectrophotometer from 4000 to 400 $cm^{-1}$ with KBr disks. Diffuse reflectance spectra (Nujol mulls) were recorded on a Shimadzu 2101-PC UV−vis instrument. UV−vis spectra of the complex solutions were recorded with an HP 8453 spectrophotometer. ESI mass (+mode) analyses were performed on a Bruker Esquire 3000 plus LC-MS system. Electronic paramagnetic resonance (EPR) spectra of molten crystals were collected with a Bruker ELEXSYS spectrometer operating at X- and Q-band frequencies. The variable-temperature magnetic susceptibility measurements were carried out on a microcrystalline sample with a Quantum Design MPMS2 SQUID susceptometer equipped with a

55 KG magnet operating at 10 KG in the range of 1.8−400 K. The susceptometer was calibrated with $[(NH_4)_2Mn(SO_4)_2]\cdot 12H_2O$.

**Synthesis of *N*-9-(toluenesulfonyl)adenine (HL) Ligand.** A solution containing 2.82 g (14.8 mmol) of *p*-toluenesulfonylchloride in dichloromethane was slowly added to a solution of 1 g of adenine (7.4 mmol) in 6 mL of pyridine under an $N_2$ atmosphere. The reaction mixture was stirred for 2 h in an ice bath. The mixture was brought to room temperature and stirred for an additional 6 h. The white solid obtained was added to 10 mL of cold water and stirred for several minutes. The solid was filtered, washed with ethanol, and dried to constant weight. Anal. HL: Calcd for $C_{12}H_{11}N_5SO_2$ (289.3): C, 49.82; H, 3.83; N, 24.21; S, 11.08. Found: C, 49.48; H, 3.83; N, 24.01; S, 10.71. $^1$H RMN (300 MHz) (DMSO-$d_6$, $\delta$/ppm): 8.6 (s, 1H, H-8); 8.2 (s, 1H, H-2); 8.0 (d, 2H, $J$(c) = 8.4 Hz, H-b); 7.6 (s, 2H, $NH_2$); 7.5 (d, 2H, $J$(c) = 8.4 Hz, H-c); 2.3 (s, 3H, $CH_3$). IR (KBr)($\nu_{max}$/ cm$^{-1}$): 3322, 3153 ($NH_2$); 1600 (C═C, C═N); 1380 ($SO_2$ asymmetric) and 1158 ($SO_2$ symmetric); 904 (S−N).

**Synthesis of $[Cu(\mu\text{-ade})(tolSO_3)(phen)]_2\cdot 2H_2O$.** A methanolic solution (30 mL) of 0.5 mmol (0.145 g) of HL containing 1 mL of $NH_3$ (35%) was added to a water solution (5 mL) of 0.25 mmol (0.5 g) of $[Cu(CH_3COO)_2]\cdot 2H_2O$. Immediately, 0.30 mmol (0.059 g) of *o*-phenanthroline were added to this mixture. The resulting dark green solution was stirred for approximately 10 min and then left to stand at room temperature. After several days, dark-green prismatic crystals suitable for X-ray diffraction were formed. Anal. Calcd for $Cu_2C_{48}H_{42}N_{14}O_8S_2$ (1134.16): C, 50.83; H, 3.73; N, 17.29; S, 5.65. Found: C, 51.05; H, 3.61; N, 17.56; S, 5.76. IR (KBr) ($\nu_{max}$/ cm$^{-1}$): 3334, 3169 ($NH_2$); 1600 (C═C, C═N); 1181 and 1159 ($SO_3$ asymmetric); 1121 ($SO_3$ symmetric). Solid-state electronic spectra ($\lambda_{max}$, nm): 420 sh, 590. UV−vis in cacodylate buffer 0.1 M (pH = 6.0) ($\lambda_{max}$, nm): 400 sh, 585 ($\epsilon$ = 57.5 M$^{-1}$cm$^{-1}$). ESI$^+$ mass spectra (cacodylate buffer 0.1 M (pH = 6.0): m/z$^+$ 302.2 ($[Cu_2(\mu\text{-ade})_2(phen)]^{2+}$, $2H_2O$); 378.3 ($[Cu_2(\mu\text{-ade})_2(phen)_2]^{2+}$); 641.1 ($[Cu_2(\mu\text{-ade})(tolSO_3)_2]^+$, $2H_2O$).

**X-ray Structure Determination for *N*-9-(toluenesulfonyl)-adenine (HL) Ligand.** A colorless crystal of HL was mounted on a glass fiber and used for data collection. Crystal data were collected at 293 K with a Nonius Kappa-CCD single-crystal diffractometer using Mo Kα radiation ($\lambda$ = 0.71073 Å). The data collection strategy was calculated with the program *COLLECT*.[31] Data reduction and cell refinement were performed with the programs *HKL DENZO* and *SCALEPACK*.[32]

The crystal structure was solved by means of direct methods with the program *SIR-97*.[33] Anisotropic least-squares refinement was carried out with *SHELXL-97*.[34] All of the non-hydrogen atoms were anisotropically refined. Some hydrogen atoms were located in a difference Fourier map and the remaining ones were located geometrically. Geometrical calculations were made with *PARST*[35] whereas the crystallographic plots were made with *ORTEP*.[36] A summary of the crystal data, experimental details, and refinement results are listed in Table S1.

**X-ray Structure Determination for $[Cu(\mu\text{-ade})(tolSO_3)(phen)]_2\cdot 2H_2O$.** A green prismatic crystal of $[Cu(\mu\text{-ade})(tolSO_3)(phen)]_2\cdot 2H_2O$ was mounted on a glass fiber and used for data collection. Crystal data were collected at 293 K with a Bruker SMART CCD 1000 diffractometer. Graphite monochromated Mo Kα radiation ($\lambda$ = 0.71073 Å) was used. The data were processed with *SAINT*[37] and corrected for absorption with *SADABS* (transmission factors = 1.000−0.772).[38]

The structure was solved by means of direct methods with the *SHELXS-97* program[39] and refined with full-matrix least-squares techniques against $F^2$ with the aid of *SHELXL-97*.[34] Positional and anisotropic atomic displacement parameters were refined for all non-hydrogen atoms. Hydrogen atoms were located on difference maps and included as fixed contributions riding on attached atoms with isotropic thermal parameters 1.2 times greater than those of their carrier atoms. The criteria for a satisfactory, complete analysis were ratios of rms shift to standard deviation of less than 0.001 and no significant features in the final difference maps. Atomic scattering factors were obtained from the International Tables for Crystallography.[40] Molecular graphics were obtained from *PLATON*[41] and *SCHAKAL*.[42] A summary of the crystal data, experimental details, and refinement results are listed in Table S1.

The crystallographic data of HL and $[Cu(\mu\text{-ade})(tolSO_3)(phen)]_2\cdot 2H_2O$ have been deposited at the Cambridge Crystallographic Data Center, CCDC numbers 643203 and 643202, respectively. Any inquiries related to the data can be e-mailed to deposit@ccdc.com.ac.uk.

**DNA−copper Complex Interaction Studies.** The fluorescence spectra were recorded with a JASCO FP-6200-spectrofluorimeter at room temperature. The experiments entailed the addition of copper(II) complex solutions at final concentrations ranging from 0 to 50 $\mu$M to samples containing 50 $\mu$M calf thymus DNA base pairs and 50 $\mu$M ethidium bromide (EB) in cacodylate buffer 0.1 M (pH = 6.0). All of the samples were excited at 500 nm, and emission was recorded between 530 and 650 nm. DNA-melting experiments were carried out by monitoring the absorbance spectrum between 1000 and 200 nm of calf thymus DNA (100 $\mu$M base pairs) at different temperatures in both the absence and the presence of the complex in ratios of 8:1, 5.5:1, and 4:1 DNA/complex. Measurements were carried out with an Agilent 8453 UV−vis spectrophotometer equipped with a Peltier temperature-controlled sample cell and driver (Agilent 89090A). The solution containing the ternary complex and CT-DNA in phosphate buffer pH = 7.2 (1 mM phosphate, 2 mM NaCl) was stirred continuously and heated with a temperature increase rate of 1 °C min$^{-1}$. The temperature interval studied ranged from 25 to 90 °C. The melting point was obtained with the first derivative using the Savitsky−Golay algorithm. Viscosity experiments were carried out with a semimicro Ubbelodhe viscosimeter immersed in a Julabo ME16G

(31) *COLLECT*, Nonius BV, 1997−2000.
(32) Otwinowski, Z.; Minor, W. DENZO-SCALEPACK: Processing of X-ray Diffraction Data Collected in Oscillation Mode. In *Methods in Enzymology*; Carter, C. W., Jr., Sweet, R. M., Eds.; Macromolecular Crystallography, part A; Academic Press: New York, 1997; Volume 276, pp 307−326.
(33) Altomare, A.; Burla, M. C.; Camalli, M.; Cascarano, G. L.; Giacovazzo, C.; Guagliardi, A.; Moliterni, A. G. G.; Polidori, G.; Spagna, R. SIR97. *J. Appl. Cryst.* **1999**, *32*, 115−119.
(34) Sheldrick, G. M. *SHELX97: Programs for Crystal Structure Analysis (Release 97−2)*; University of Göttingen: Göttingen, Germany, 1997.
(35) (a) Nardelli, M. PARST. *Comput. Chem.* **1983**, *7*, 95−97. (b) Nardelli, M. J. *Appl. Crystallogr.* **1995**, *28*, 659.
(36) Farrugia, L. J. ORTEP3 for Windows. *J. Appl. Cryst.* **1997**, *30*, 565.
(37) Bruker. *SMART* and *SAINT*. *Area Detector Control and Integration Software*; Bruker Analytical X-ray Instruments Inc.: Madison, WI, 1997.
(38) Sheldrick, G. M. *SADABS*. *Program for Empirical Absorption Correction of Area Detector Data*; University of Göttingen: Göttingen, Germany, 1997.
(39) Sheldrick, G. M. *Acta Cryst.* **1990**, *A46*, 467−473.
(40) Wilson, A. J. C. International Tables for Crystallography. Vol. C, Kluwer Academic Publishers: Dordrecht, The Netherlands, 1995.
(41) Spek, A. L. *PLATON*. *A Multipurpose Crystallographic Tool*; Utrecht University, Utrecht, The Netherlands, 2003.
(42) Keller, E. *SCHAKAL-97*. *A computer program for the graphic representation of molecular and crystallographyc models*; University of Freiburg i. Br.: Freiburg, Germany, 1997.

thermostatted bath maintained at 37.0 ± 0.1 °C. Solutions of the complexes (final concentrations ranging from 1 to 10 $\mu$M) in cacodylate buffer 0.1 M (pH = 6.0) were added to a solution of calf thymus DNA (50 $\mu$M base pairs) in cacodylate buffer. The flow times were measured in triplicate with a stopwatch. Data were presented as $(\eta/\eta_0)^{1/3}$ versus the ratio of the complex concentration to DNA, where $\eta$ is the viscosity of the DNA in the presence of the complex and $\eta_0$ is the viscosity of the DNA alone. Viscosity values were calculated from the observed flow time of a DNA-containing solution corrected from the flow time of buffer alone ($t_0$), $\eta = t - t_0$.

**DNA Cleavage.** Reactions were performed by mixing 7 $\mu$L of cacodylate buffer, 6 $\mu$L of complex solution (with final concentrations of 3, 6, 9, and 12 $\mu$M), 1 $\mu$L of pUC18 DNA solution (0.25 $\mu$g/$\mu$l, 750 $\mu$M in base pairs), and 6 $\mu$L of activating agent solution (sodium ascorbate or 3-mercaptopropionic acid) in a 2.5-fold molar excess relative to the concentration of the complex. The resulting solutions were incubated for 1 h at 37 °C, after which time a quench buffer solution (3 $\mu$L) consisting of bromophenole blue (0.25%), xylene cyanole (0.25%), and glycerol (30%) was added. The solution was then subjected to electrophoresis on 0.8% agarose gel in 0.5X TBE buffer (0.045 M Tris, 0.045 M boric acid, and 1 mM EDTA) containing 2 $\mu$L/100 mL of a solution of EB (10 mg/mL) at 80 V for 2 h. The bands were photographed on a capturing system (Gelprinter Plus TDI).

The kinetic study of the cleavage was performed at different times with plasmid pUC18, which was incubated at 37 °C with 9 $\mu$M complex and 22.5 $\mu$M ascorbate. Samples were treated as described above. The relative amounts of different plasmid structures were quantified with the aid of ImageJ 1.34s.[43] A correction factor of 1.3 was used for the assessment of supercoiled DNA (Form I) because the intercalation between EB and Form I DNA is relatively weak compared to that of nicked (Form II) and linear (Form III) DNA.[44] All of the results are the average of experiments performed in triplicate. Kinetic profiles were fitted to first-order process models with the program Origin 7.5. The $t_{1/2}$ value was calculated using the equation $t_{1/2} = -\ln(0.5)/k_{obs}$.

To test for the presence of reactive oxygen species (ROS) generated during strand scission and for possible complex−DNA interaction sites, various reactive oxygen intermediate scavengers and groove binders were added to the reaction mixtures. The scavengers used were 2,2,6,6-tetramethyl-4-piperidone (0.4 M), 1,4-diazabicyclo[2,2,2]octane (DABCO) (0.4 M), Tiron (10 mM), sodium formiate (0.4 M), potassium iodide (0.4 M), DMSO (0.4 M), urea (0.4 M), and catalase 10 $\mu$g/mL (650 U/mL). In addition, a chelating agent of copper(I), neocuproine (36 $\mu$M), along with the groove binders methyl green (3 $\mu$M) and distamycin (8 $\mu$M) were also assayed. Samples were treated as described above.

## Results and Discussion

The reaction of $[Cu(CH_3COO)_2]\cdot 2H_2O$ with *N*-9-(toluenesulfonyl)adenine (HL) (Chart 1) in methanolic ammonia solution leads to the hydrolysis of HL to give adeninate and toluenesulfonate anions that coordinate Cu(II), thus affording the dinuclear complex $[Cu(\mu\text{-ade})(tolSO_3)(phen)]_2\cdot 2H_2O$.

**Crystal Structure of *N*-9-(toluenesulfonyl)adenine (HL).** The geometry of one of the three molecules that form the asymmetric unit is shown in Figure S1. The interatomic distances and bond angles are given in Table S2. Bond distances and angles for all three molecules are nearly equivalent. The structural parameters in the purine ring are similar to those described for the adenosine nucleoside.[45] The environment of the S atom is that of a distorted tetrahedron, which is common in the sulfonamides as a result of the nonbinding interactions between the S=O bonds.[46] The crystal structure is stabilized with hydrogen bonds between two HL molecules. Both ligands form a self-base pair through two moderate hydrogen bonds[47] formed by the N atoms of the heterocyclic ring and the amine group.

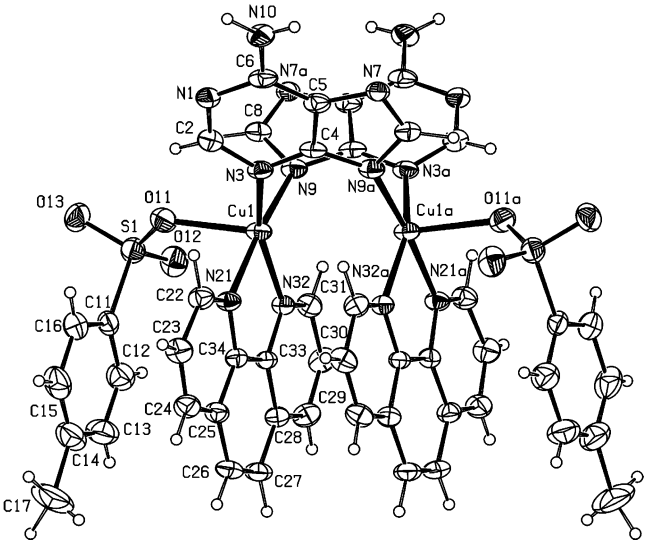


**Figure 1.** *ORTEP* drawing of $[Cu(\mu\text{-ade})(tolSO_3)(phen)]_2\cdot 2H_2O$.

**Table 1.** Selected Bond Distances (Angstroms) and Angles (Degrees) for $[Cu(\mu\text{-ade})(tolSO_3)(phen)]_2\cdot 2H_2O$[a]

| distances (Å) | | angles (°) | |
|---|---|---|---|
| Cu1−N9#1 | 1.993(3) | N3−Cu1−N9#1 | 90.03(13) |
| Cu1−N3 | 1.991(3) | N9#1−Cu1−N32 | 95.34(13) |
| Cu1−N21 | 2.062(3) | N32−Cu1−N21 | 80.53(12) |
| Cu1−N32 | 2.019(3) | N21−Cu1−N3 | 92.86(12) |
| Cu1−O11 | 2.206(3) | N3−Cu1−O11 | 100.85(13) |
| | | N9#1−Cu1−O11 | 94.30(13) |
| Cu1−Cu1#1 | 3.2473(10) | N32−Cu1−O11 | 98.52(12) |
| | | N21−Cu1−O11 | 89.23(12) |
| | | N3−Cu1−N32 | 159.44(14) |
| | | N9#1−Cu1−N21 | 174.95(13) |
| | | N3−Cu1−N9#1 | 90.03(13) |
| | | N9#1−Cu1−N32 | 95.34(13) |

[a] Symmetry transformation used to generate equivalent atoms: (#1) $-x + 1, y, -z + 1/2$.

**Description of the Crystal Structure of $[Cu(\mu\text{-ade})(tolSO_3)(phen)]_2\cdot 2H_2O$.** The *ORTEP* drawing of the $[Cu(\mu\text{-ade})(tolSO_3)(phen)]_2\cdot 2H_2O$ complex with the atomic numbering scheme is shown in Figure 1. The relevant structural parameters for the compound are listed in Table 1. The structure consists of a dimeric unit with a *C*2 symmetry axis, where both coppers are bridged by two adeninate anions. Each copper atom of the dinuclear entity

(43) Wayne Rasband, ImageJ 1.34s. National Institutes of Health, U.S.A.
(44) Hertzberg, R. P. *J. Am. Chem. Soc.* **1982**, *104*, 313−315.
(45) Saenger, W. *Principles of Nucleic Acid Structure*; Springer-Verlag: New York, 1984.
(46) Cejudo-Marín, R.; Alzuet, G.; Ferrer, S.; Borrás, J. *Inorg. Chem.* **2004**, *43*, 6805−6814.
(47) Jefrey, G. A. *Introduction to Hydrogen Bonding*; Oxford University Press: Oxford, U.K., 1997.

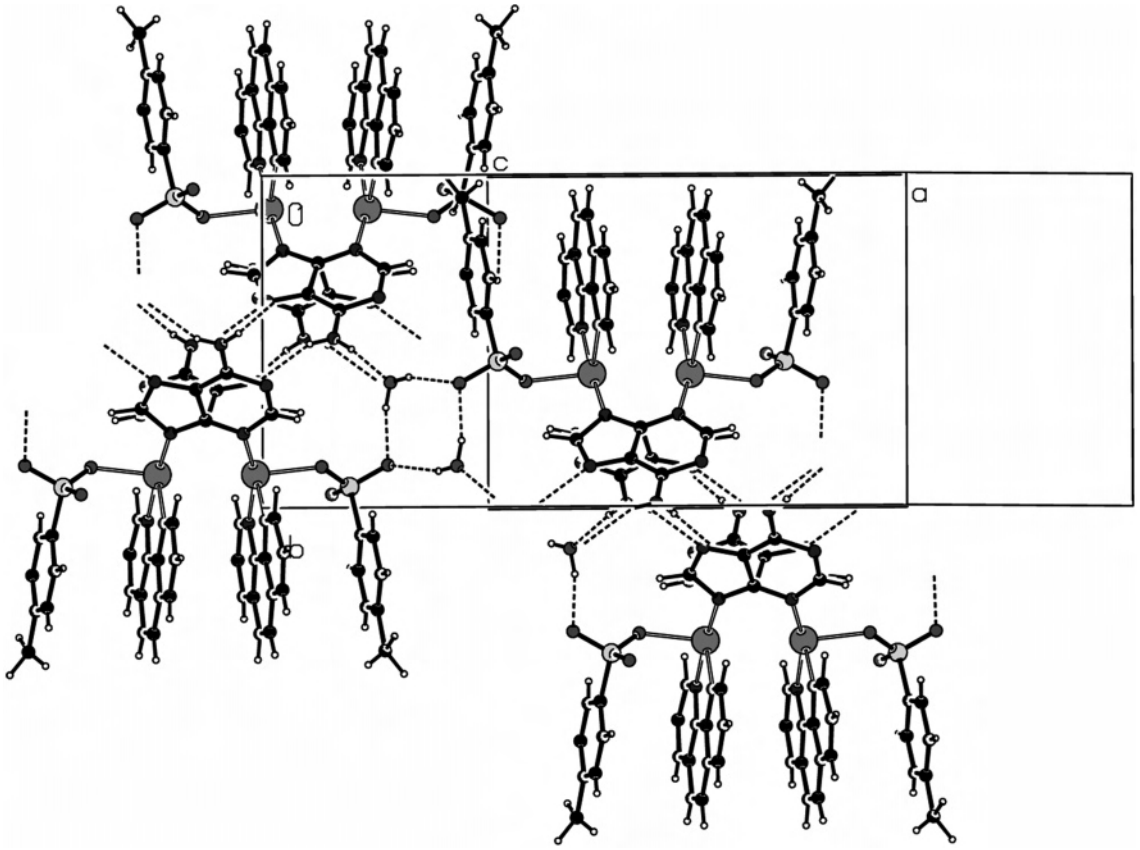


**Figure 2.** Crystal packing of $[Cu(\mu\text{-ade})(tolSO_3)(phen)]_2 \cdot 2H_2O$ showing $\pi-\pi$ interactions and hydrogen bonds.

is five-coordinated. A $\tau$ value of 0.26 indicates a distorted square pyramidal geometry. The copper(II) ions are linked to two N atoms of a phenanthroline molecule [Cu−N(21) = 2.062(3) Å and Cu−N(32) = 2.019(3) Å], to the N3 of one adeninate ligand [Cu−N(3) = 1.991(3) Å], and to the N(9)#1 of another adeninate ligand [Cu−N(9)#1 = 1.993-(3) Å]. The Cu−N distances are similar to those found in previously reported copper−phenanthroline and copper−adeninate complexes.[8,48,49] These N atoms form the equatorial plane; the copper(II) ion deviates from this plane by 0.2026 Å. The apical position is occupied by one sulfonate oxygen atom [Cu−O(11) = 2.206(3) Å]. The Cu−O(11) bond distance is longer than the equatorial bond distances, partly because the fifth coordination position in square pyramidal arrangements is usually longer,[50,51] but also partly because of the low coordination capability of the toluenesulfonate anion. The observed $Cu-O_{sulfonate}$ distance is equivalent to those in the ternary complexes Cu−phenanthroline−sulfonate.[52] The two copper atoms are bridged by two NCN groups of deprotonated adenine ligands, with the metallic centers separated by a distance of 3.2473(10) Å. This distance is longer than those typically found in dinuclear copper complexes with four adenine ligands as bridges,[53] a fact which may be attributed to the presence of only two bridges. The N−Cu−N angles range from 80.53(12) to 95.34(13) degrees. The smaller angle corresponds to that formed by the copper ion and two N phenanthroline atoms, as is common in copper−phenanthroline complexes.[54−56] This particular compound is noteworthy because of the presence of $\pi-\pi$ interactions brought on by intramolecular parallel stacking between the phenanthroline ligands as well as between the toluenesulfonate ring and the closest neighboring phenanthroline molecule (Figure 2). The geometric parameters for these $\pi-\pi$ interactions are summarized in Table 2. In addition, the structure is stabilized by an intramolecular hydrogen bond between the O(1) of a water molecule and the O(13) belonging to the sulfonate group, as well as by intermolecular hydrogen bonds with adjacent adeninate anions (Table 3) (Figure 2). All of the hydrogen bonds are of moderate strength.[47] The hydrogen bonds between N(7) and N(10) of the two adeninate ligands give rise to adenine

(48) Zhang, S.; Zhu, Y.; Tu, C.; Wei, H.; Yang, Z.; Lin, L.; Ding, J.; Zhang, J.; Guo, Z. *J. Inorg. Biochem.* **2004**, *98*, 2099−2106.
(49) Sánchez-Moreno, M. J.; Choquesillo-Lazarte, D.; González-Pérez, J. M.; Carballo, R.; Castiñeiras, A.; Niclós-Gutierrez, J. *Inorg. Chem. Comm.* **2002**, *5*, 800−802.
(50) Murase, I.; Vuckovic, G.; Kodera, M.; Harada, H.; Matsumoto, N.; Kida, S. *Inorg. Chem.* **1991**, *30*, 728−733.
(51) Bailey, N. A.; Fenton, D. E.; Franklin, M. V.; Hall, M. *J. Chem. Soc., Dalton Trans.* **1980**, 984−990.
(52) Yang, J.; Ma, J.-F.; Wu, D.-M.; Guo, L.-P.; Liu, J.-F. *J. Mol. Struct.* **2003**, *657*, 333−341.
(53) Sonnenfroh, D.; Kreilick, W. *Inorg. Chem.* **1980**, *19*, 1259−1262.
(54) Patel, R. N.; Singh, N.; Shukla, K. K.; Niclós-Gutiérrez, J.; Castiñeiras, A.; Vaidyanathan, V. G. *Spectrochim. Acta, Part A* **2005**, *62*, 261−268.
(55) Morehouse, S. M.; Suliman, H.; Haff, J.; Nguyen, D. *Inorg. Chim. Acta* **2000**, *297*, 411−416.
(56) Matovic, Z. D.; Pelosi, G.; Lanelli, S.; Ponticelli, G.; Radanovic, D. D.; Radanovic, D. J. *Inorg. Chim. Acta* **1998**, *268*, 221−230.

**Table 2.** Geometric Parameters for $\pi-\pi$ Stacking $[Cu(\mu\text{-ade})(tolSO_3)(phen)]_2 \cdot 2H_2O$[a]

| $\pi-\pi$ stacking | $d_{C-C}$ (Å) | $\alpha$ (°) | $\beta$ (°) | $\gamma$ (°) | $d_\perp$[Cg(J) − P(J)](Å) | $d_\perp$[Cg(J) − P(I)] (Å) |
|---|---|---|---|---|---|---|
| | | | phen−phen | | | |
| Cg(5)-Cg(6)[b] | 3.5621 | 8.16 | 21.03 | 20.47 | 3.337 | 3.325 |
| Cg(6)-Cg(8)[b] | 3.6900 | 6.64 | 20.20 | 25.02 | 3.344 | 3.463 |
| Cg(8)-Cg(8)[b] | 3.7223 | 6.66 | 21.63 | 21.63 | 3.460 | 3.460 |
| | | | $tolSO_3$-phen | | | |
| Cg(7)-Cg(5) | 3.7460 | 2.48 | 20.57 | 22.69 | 3.456 | 3.507 |
| Cg(7)-Cg(8) | 3.6059 | 2.75 | 17.71 | 16.27 | 3.461 | 3.435 |

[a] $d_{C-C}$: centroids distance; $\alpha$: dihedral angle between the rings; $\beta$, $\gamma$: slipping angles; $d_\perp$[Cg(I)-P(J)] and $d_\perp$[Cg(J)-P(I)]: centroid Cg(I) to plane J distance and the opposite. [b] $1-x, y, {}^1/_2 - z$. (Cg(5): N21−C22−C22−C24−C25−C34, Cg(6): N32−C33−C28−C29−C30−C31, Cg(7): C11−C12−C13−C14−C15−C16, Cg(8): C25−C26−C27−C28−C33−C34).

**Table 3.** Hydrogen Bonds in $[Cu(\mu\text{-ade})(tolSO_3)(phen)]_2 \cdot 2H_2O$[a]

| D−H···A | d(D−H) (Å) | d(H···A) (Å) | d(D···A) (Å) | DHA (°) |
|---|---|---|---|---|
| N10−H10A···N7#2 | 0.83 | 2.27 | 3.049 | 156.2 |
| N10−H10B···O1#3 | 0.95 | 2.01 | 2.947 | 167.1 |
| O1−H1A···O13 | 0.68 | 2.30 | 2.923 | 151.9 |
| O1−H1B···O13#4 | 0.85 | 2.02 | 2.845 | 161.7 |

[a] Symmetry codes: #2 $-x+1, -y+2, -z+1$; #3 $-x+{}^1/_2, y+{}^1/_2, -z+{}^1/_2$; #4 $-x+{}^1/_2, -y+{}^3/_2, -z$.

homodimers such as $A_1A_1$, according to the classification by Kelly et al.[57]

**IR Spectrum.** The IR spectrum of the Cu(II) complex shows the characteristic bands of adenine. The $\nu(NH_2)$ asymmetric and symmetric vibrations appear at 3334 and 3169 $cm^{-1}$, respectively. The $\delta(NH_2)$ is found at 1666 $cm^{-1}$. The $\nu$(C═C) and $\nu$(C═N) vibrations of the heterocyclic ring are observed as a broad band centered at 1600 $cm^{-1}$,[3] which must also include the corresponding vibrations of the phenanthroline ligand. With respect to the typical vibrations of the toluenesulfonate group, the $\nu(SO_3)_{asym}$ appears as a doublet at 1181 and 1159 $cm^{-1}$, which indicates a coordination with the copper ion, whereas the $\nu(SO_3)_{sym}$ band can be appreciated at 1121 $cm^{-1}$.[52] The bands at 1228 and 850 $cm^{-1}$ can be attributed to phenanthroline ring vibrations.[58]

**Diffuse Reflectance and UV−vis Spectra.** The solid-state Nujol mull transmittance electronic spectrum exhibits a broad band with a maximum of about 590 nm (16 950 $cm^{-1}$), probably due to a d−d transition and consistent with a $CuN_4O$ chromophore.[59] This spectrum also shows a shoulder at ca. 420 nm (23 800 $cm^{-1}$), which is attributed to a LMCT transition. The similarity of the UV−vis spectrum in cacodylate buffer 0.1 M (pH = 6.0) with a band at 585 nm and a shoulder at 400 nm indicates that the chromophore remains in solution. The proposed stability of the compound is corroborated by the ESI results, which show that the two copper(II), two adeninate, and two phenanthroline species exist as a whole entity.

**Magnetic Properties.** Magnetic susceptibility measurements of $[Cu(\mu\text{-ade})(tolSO_3)(phen)]_2 \cdot 2H_2O$ were performed on crystals in the temperature range of 2−270 K. The temperature dependence of the magnetic susceptibility is shown in Figure 3. The dominant features of the plot include

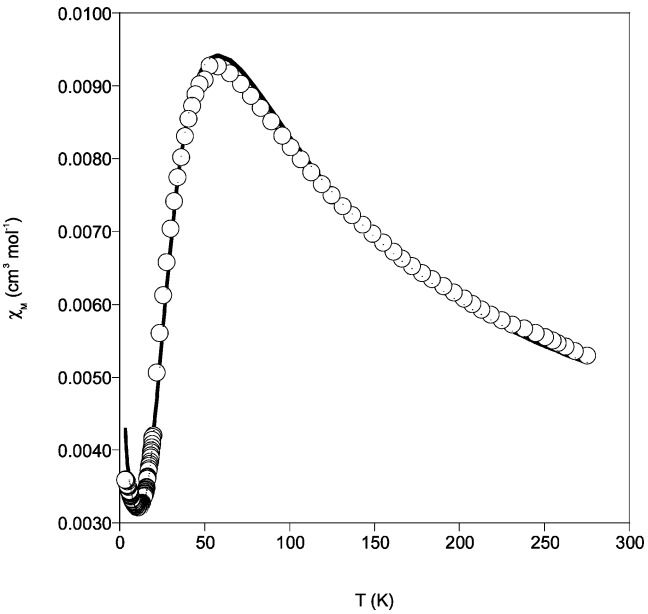


**Figure 3.** Temperature dependence of $\chi_M$ for $[Cu(\mu\text{-ade})(tolSO_3)(phen)]_2 \cdot 2H_2O$. The solid line represents the fitted function.

a maximum around 50 K and a rapid decrease to zero at lower temperatures. The solid curve in Figure 3 is the best fit of the data to the Bleaney−Bowers equation:[60]

$$\chi_M = (Ng^2\beta^2/kT)[3 + \exp(-2J/kT)]^{-1}(1-\rho) + \rho Ng^2\beta^2/4kT + \chi_{TIP}$$

which results from a consideration of the eigenvalues of $\hat{H} = -2J\hat{S}1\hat{S}2$ and where the symbols have the usual meanings. A good fit was obtained when $-2J = 65$ $cm^{-1}$, $g = 2.06$, $\chi_{TIP} = 2.59 \cdot 10^{-3}$, $\rho = 0.013$, and $R = 9 \cdot 10^{-4}$ ($R = 10^{-3}\Sigma(\chi \text{ exptl} - \chi \text{ calcd})^2T^2$).

The antiferromagnetic coupling constant for the complex is lower than that of other complexes with four NCN adeninate bridges, which generally present coupling constants for $-2J$ between 179 and 285 $cm^{-1}$.[53] The lower $-2J$ value for our compound is probably due to the fact that only two adeninate bridges are present; however, other factors can also affect the exchange coupling constant. For example, Sonnenfroh and Kreilick[53] found that the observed exchange energies for this type of compounds vary systematically with the charge of the purine rings and axial ligands. Thus, the

(57) Kelly, R. E. A.; Lee, Y. J.; Kantorovich, L. N. *J. Phys. Chem. B* **2005**, *109*, 11933−11939.
(58) Calatayud, M. L.; Sletten, J.; Julve, M.; Castro, I. *J. Mol. Structure* **2005**, *741*, 121−128.
(59) Cabras, M. A.; Zoroddu, M. A. *Inorg. Chim. Acta* **1987**, *136*, 17−19.
(60) Bleaney, B.; Bowers, K. D. *Proc. R. Soc. London, Ser. A* **1952**, *214*, 451−465.

complexes with adeninate bridging ligands present less exchange interaction than the complexes with adenine bridging ligands. Moreover, whereas variation of the axial ligands should have little effect on mechanisms involving exchange through the ligands themselves, such variation does exert an effect on the relative energy separations of the $d_{x^2-y^2}$ and $d_{z^2}$ orbitals of the metals. These authors thus observed that complexes in which $H_2O$ was the axial ligand presented more tetragonal distortion than similar complexes with piperidine and ammonia. As a result, there was a larger separation between the $d_{x^2-y^2}$ and $d_{z^2}$ levels. In our study, the axial O sulfonate atom of the title compound gives rise to a more tetragonal distortion; therefore, the $d_{x^2-y^2}$ and $d_{z^2}$ levels present a larger separation than that of the complex with the water ligand. To some extent, then, this factor also contributes to the low $-2J$ value of $[Cu(\mu\text{-ade})(tolSO_3)(phen)]_2 \cdot 2H_2O$.

**Electronic Paramagnetic Resonance.** The EPR spectra of the complex obtained at the X and Q bands (Figure 4) show signals typical for coupled dinuclear complexes,[61,62] together with the characteristic signal of a monomeric species at ~3300 G (Figure 4a) and ~11 400 G (Figure 4b). The formation of a dinuclear complex is connected with the antiferromagnetic coupling of two Cu(II) ions, leading to a singlet ground state and an excited spin triplet state. The energy difference between these states, expressed as $2J$, depends on the strength of the interaction. If the triplet state is thermally accessible ($2J \approx KT \approx 200-400$ cm$^{-1}$), then paramagnetism is observed, which allows for the adequate description of the EPR spectra through the interactive spin Hamiltonian for isolated Cu(II) dimers ($S = 1$).[46] In the case of copper dimers with axial symmetry when $D < h\nu$, four resonance fields can be determined ($H_{z1}$, $H_{xy1}$, $H_{xy2}$, and $H_{z2}$), along with a forbidden transition ($\Delta m_s = \pm 2$). The X-band EPR spectrum (Figure 4a) shows transitions at 2322, 2820, and 3827 G, which are assigned to the resonance fields $H_{z1}$, $H_{xy1}$, and $H_{xy2}$, respectively. In the Q-band spectrum, these signals appear at 10 016, 11 300, and 12 265 G. The $H_{z2}$ transition is not observed in either case. The formally forbidden half-field spin transition ($\Delta m_s = \pm 2$) is observed at 1591 and 5800 G in the X- and Q-band spectra, respectively.

From the observed transitions $H_{z1}$, $H_{xy1}$, $H_{xy2}$ and the half-field spin transition,[63] the calculated parameters are as follows: $D = 0.0970$ cm$^{-1}$, $g_{||} = 2.190$, and $g\perp = 2.023$. This $D$ value is slightly smaller than those of related complexes with purine ligands.[53] The $g$ value calculated from the expression $g = {}^1/_3(g_{||} + g\perp)$ is 2.07, similar to that obtained with the mathematical fitting of the experimental susceptibility data ($g = 2.06$). The observed $D$ value is expressed as $D_{obs} = D_{dd} + D_{exch}$, where $D_{dd}$ and $D_{exch}$ arise from dipole−dipole and exchange interactions, respectively. $D_{dd}$, which should be negative, has been approximately

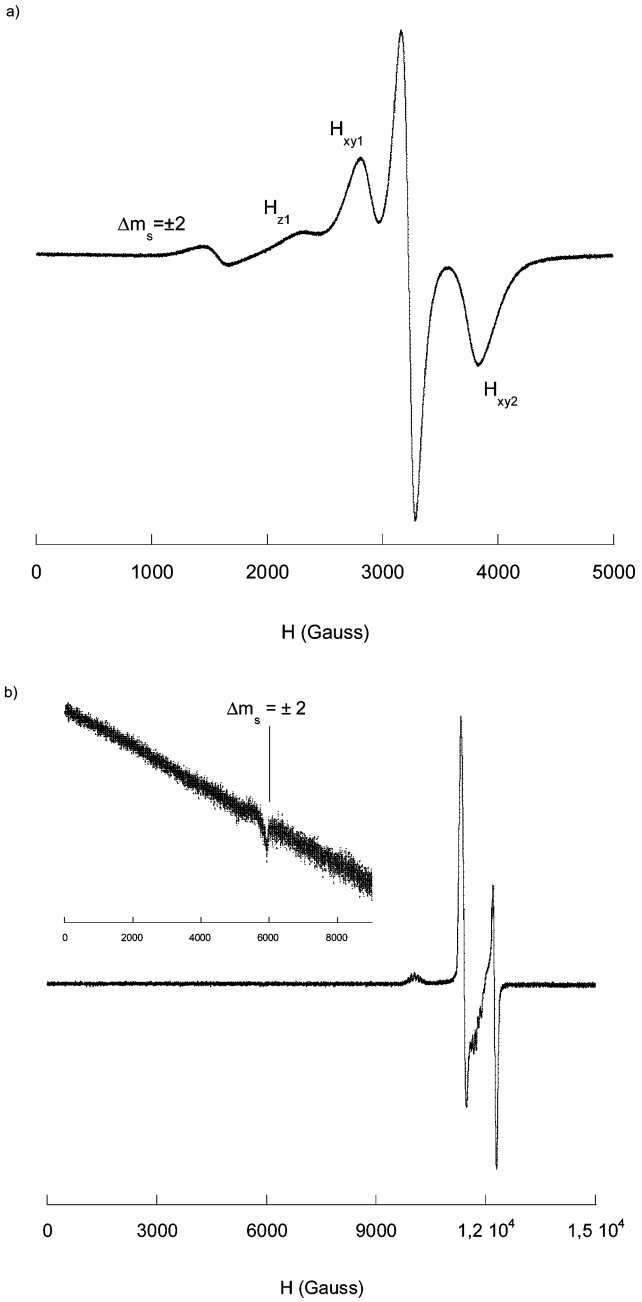


**Figure 4.** (a) X-band powder EPR spectrum of $[Cu(\mu\text{-ade})(tolSO_3)(phen)]_2 \cdot 2H_2O$ at room temperature. (b) Q-band powder EPR spectrum of $[Cu(\mu\text{-ade})(tolSO_3)(phen)]_2 \cdot 2H_2O$ at 20 K.

calculated[64] from the equation based on a point dipole model, $R^3 = 0.65\, g_z^2/D_{dd}$, where $R$ is the copper−copper distance. Application of this equation gives $D_{dd} = 0.0911$ cm$^{-1}$ and, in turn, $D_{exch} = 0.1885$ cm$^{-1}$. Rough correlations between $D_{exch}$ and $2J$ have been made with the equation $D_{exch} = -2J[((g_z - 2)^2/4) - (g_{xy} - 2)^2]/8$.[65] From this equation, a value of $-2J = 177.49$ cm$^{-1}$ is obtained, whereas the experimental value is 65 cm$^{-1}$. The difference between the calculated and the experimental values may be due to the approximations made in deriving the equations and also to the fact that the singlet−triplet splitting is not simply related

(61) Wasson, J. R.; Shyr, Chin-I.; Trapp, C. *Inorg. Chem.* **1968**, *7*, 469−473.
(62) Wasserman, E.; Snyder, L. C.; Yager, W. A. *J. Chem. Phys.* **1964**, *41*, 1763−1772.
(63) Eaton, S. A.; More, D. M.; Sawant, B. M.; Eaton, G. R. *J. Am. Chem. Soc.* **1983**, *105*, 6560−6567.
(64) Chastteen, N. D.; Belford, R. L. *Inorg. Chem.* **1970**, *9*, 169−175.
(65) Ruiz, E.; Cano, J.; Alvarez, S.; Alemany, P. *J. Comput. Chem.* **1999**, *20*, 1391−1400.

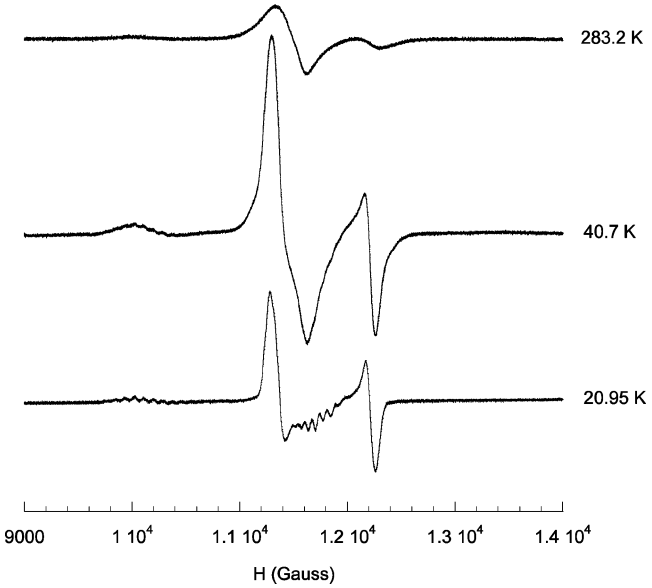


**Figure 5.** Q-band powder EPR spectra of $[Cu(\mu\text{-ade})(tolSO_3)(phen)]_2 \cdot 2H_2O$ at 283.2, 40.7, and 20.95 K.

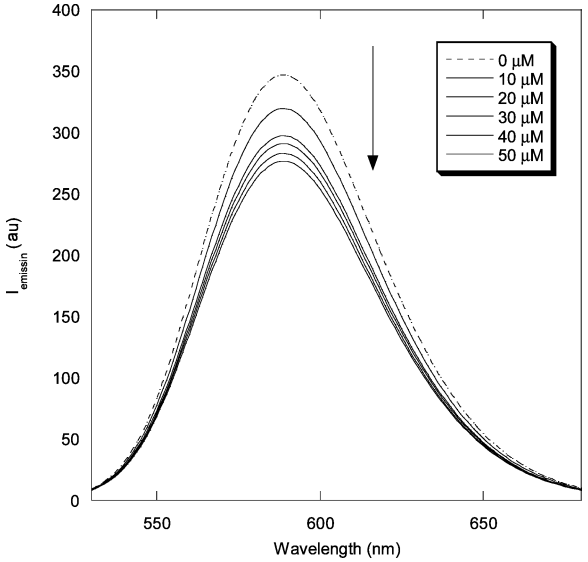


**Figure 6.** Emission spectra of EB bound to DNA in the absence (dotted line) and presence (continuous lines) of $[Cu(\mu\text{-ade})(tolSO_3)(phen)]_2 \cdot 2H_2O$. The arrow shows the changes in intensity at increasing concentrations of the complex.

to the strength of the exchange interaction, as has been pointed out elsewhere.[66]

The EPR spectrum at the Q band was recorded at different temperatures (Figure 5). At 10 K, the EPR was silent. At 283.2 K, the peaks were clearly much broader than those at 40.7 K. This is due to two main factors: first, triplet states are relatively more populated, and second, relaxation times ($T_{1e}$) are shorter at higher temperatures. These circumstances both lead to intermolecular interactions. When the temperature decreased to 20.95 K, the spectrum became narrower and seven hyperfine features with a relative intensity of 1:2:3:4:3:2:1 were observed in the low-field components. This is due to the two interacting Cu(II) ions ($2nI + 1$; $n = 2$ and $I = {}^3/_2$). The separation between these signals is approximately 67 G, representing just half of the hyperfine splitting evident on the line corresponding to the free copper ion. This is exactly what is to be expected from a line originating from an exchange interaction.[67]

**DNA Binding Properties.** Because DNA is the primary pharmacological target of many antitumor compounds,[68] the interaction between DNA and metal complexes is of paramount importance in understanding the mechanism of tumor inhibition for the treatment of cancer. Thus, the mode of and propensity for binding of the complex to calf thymus DNA (CT-DNA) was studied with the aid of different techniques.

**Fluorescence Spectroscopic Studies.** Ethidium bromide (EB) emits intense fluorescent light when it is intercalated between adjacent DNA base pairs. The addition of a second DNA-binding molecule can quench the DNA-EB adduct emission by either replacing the EB and/or by accepting the excited-state electron of the EB through a photoelectron transfer mechanism.[69,70] Figure 6 shows the emission spectra of EB bound to DNA in both the absence and presence of the copper(II) complex at increasing concentrations. Addition of the compound to DNA that has been previously treated with EB causes an appreciable reduction in emission intensity, thus indicating that the complex binds to DNA.

**Thermal Denaturation.** The binding of the complex to CT-DNA was also studied by examining the thermal denaturation profile of DNA. The melting temperature ($T_m$) of DNA characterizes the transition from double-stranded to single-stranded nucleic acid.[71] When added to DNA in increasing concentrations, $[Cu(\mu\text{-ade})(tolSO_3)(phen)]_2 \cdot 2H_2O$ produced an increase in $T_m$ (Figure 7). The stabilization of the DNA double helix by binding of the copper(II) complex increased when the molar ratio of compound to DNA was incremented. The observation of monophasic melting curves with a high $\Delta T_m$ value (21.6 °C) for [DNA]/[complex] = 4 suggests that the copper complex is involved in the strong stabilization of duplex DNA.

**Viscosimetry Studies.** Hydrodynamic measurements that are sensitive to length changes are regarded as the least ambiguous and the most critical tests of a DNA binding model in solution, providing reliable evidence for the DNA binding mode. One classic intercalation model results in the lengthening of the DNA helix as the base pairs are separated to accommodate the binding ligand, thus leading to an increase in DNA viscosity. In contrast, complexes that bind exclusively in DNA grooves by means of partial and/or nonclassic intercalation under the same conditions typically cause either a less pronounced change (positive or negative) in DNA solution viscosity or none at all.[72] Our results (data not shown) reveal that the compound has no effect on the

(66) Gutiérrez, L.; Alzuet, G.; Borrás, J.; Castiñeiras, A.; Rodríguez-Fortea, A.; Ruiz, E. *Inorg. Chem.* **2001**, *40*, 3089−3096.
(67) Slichter, C. P. *Phys. Rev.* **1955**, *99*, 479−480.
(68) Quiroga, A. G.; Perez, J. M.; Lopez-Solera, I.; Montero, E. I.; Masaguer, J. R.; Alonso, C.; Navarro-Raninger, C. *J. Inorg. Biochem.* **1998**, *69*, 275−281.
(69) Baguley, B. C.; Le Bret, M. *Biochemistry* **1984**, *23*, 937−943.
(70) Selvakumar, B.; Rajendiran, V.; Uma Maheswari, P.; Stoeckli-Evans, H.; Palaniandavar, M. J. *Inorg. Biochem.* **2006**, *100*, 316−330.
(71) Tselepi-Kalouli, E. T.; Katsaros, N. *J. Inorg. Biochem.* **1989**, *37*, 271−282.

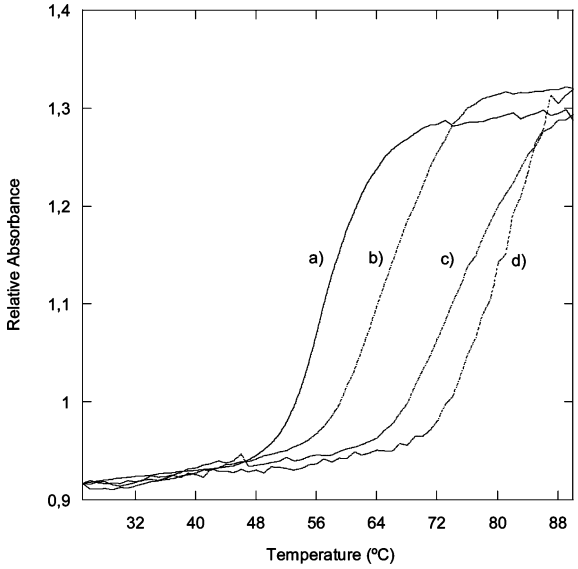


**Figure 7.** DNA melting temperature dependence on complex concentration. (a) CT-DNA 100 $\mu$M in the absence of the complex. (b), (c), and (d) CT-DNA 100 $\mu$M in the presence of 12.5 $\mu$M, 18 $\mu$M, and 25 $\mu$M of the complex, respectively.

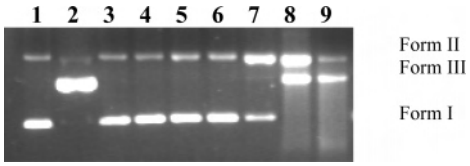


**Figure 8.** Agarose gel electrophoresis of pUC18 plasmid DNA treated with $CuSO_4 \cdot 5H_2O$ or the complex in the presence of ascorbate. [ascorbate]/[complex] = 2.5:1. Incubation time 1 h (37 °C). Lane 1, supercoiled DNA; Lane 2, lineal DNA; Lane 3, DNA + ascorbate 30 $\mu$M; Lane 4, $CuSO_4 \cdot 5H_2O$ 12 $\mu$M (ascorbate 15 $\mu$M); Lane 5, $CuSO_4 \cdot 5H_2O$ 24 $\mu$M (ascorbate 30 $\mu$M); Lane 6, complex 3 $\mu$M (ascorbate 7.5 $\mu$M); Lane 7, complex 6 $\mu$M (ascorbate 15 $\mu$M); Lane 8, complex 9 $\mu$M (ascorbate 22.5 $\mu$M); Lane 9, complex 12 $\mu$M (ascorbate 30 $\mu$M).

relative viscosity of CT-DNA. These findings indicate that the interaction does not involve a classic intercalation and that the compound probably binds either in DNA grooves or in the sugar−phosphate backbone.

**Nuclease Activity of the Complex.** The ability of the title complex to cleave DNA has been studied with the aid of gel electrophoresis of supercoiled pUC18 DNA in cacodylate buffer (pH = 6.0) with ascorbate.

The complex was found to perform DNA cleavage in a concentration-dependent manner. The results given in Figure 8 indicate that the complex is a potent chemical nuclease with higher nuclease activity than copper sulfate. Indeed, at the very low concentration of 6 $\mu$M, the compound was capable of mediating the conversion of supercoiled DNA to its open circular form (lane 7). At 9 $\mu$M, the compound induced complete degradation of the supercoiled form to produce the open circular and linear forms and small linear fragments (lane 8). At 12 $\mu$M, the open circular form III was transformed into small linear fragments, and a considerable smear appeared (lane 9). In the control experiment, two equivalents of copper sulfate did not exert DNA scission activity (lanes 4 and 5). This last result suggests that a possible synergistic effect may exist between the two copper(II) ions, which, in turn, contributes to the complex's relatively high nucleolytic efficiency.[20,21,73]

The nuclease efficiency of copper(II) complexes is usually dependent on the activators employed.[74−76] Thus, in addition to ascorbate, we also used 3-mercaptopropionic acid (MPA) to investigate the compound's ability to cleave DNA (Figure S2). We found that while the compound also behaves as a nuclease in the presence of MPA, its efficacy is significantly lower than it is in the presence of ascorbate.

Because the compound contains 1,10-phenanthroline as a ligand, we decided to compare its nucleolytic activity with that of bis(*o*-phenanthroline)copper complex, which is a well-known and very efficient chemical nuclease. Figure S3 shows that at 6 $\mu$M, the title complex is a more efficient chemical nuclease than the latter complex at the same concentration. In summary, the complex exhibited remarkable DNA cleavage activity with both MPA and ascorbate.

**Kinetic Study of DNA cleavage by $[Cu(\mu\text{-ade})(tolSO_3)(phen)]_2 \cdot 2H_2O$.** The kinetic parameters underlying the chemistry of the complex's ability to cleave DNA were determined by following the time dependence of the reaction under pseudo-first-order conditions ([complex] = 9 $\mu$M and [DNA] = 37.5 $\mu$M in bp). The loss of supercoiled DNA and increased levels of open circular and linear DNA forms were quantified after gel electrophoresis, as described in the Experimental Section, and then fitted with the aid of the kinetic model proposed by Hughes et al.[77] This model contemplates two consecutive and independent first-order processes in which form II is produced from form I ($k_{obs1}$) and then cleaved to form III ($k_{obs2}$). The results are shown in Figure 9. $[Cu(\mu\text{-ade})(tolSO_3)(phen)]_2 \cdot 2H_2O$ was found to mediate the cleavage of one strand of dsDNA in the initial stage of the reaction. Subsequent nicking was also promoted by the compound, resulting in the formation of linear DNA. At 60 min (lane 11, Figure 9a), the complex cleaved the DNA, producing some smearing in the process. The reaction profile for the $[Cu(\mu\text{-ade})(tolSO_3)(phen)]_2 \cdot 2H_2O$-mediated DNA cleavage displayed pseudo-first-order kinetic behavior (Figure 9b), with $k_{obs1} = \sim 0.141\ min^{-1}$ and $R^2 = 0.99$. The half-life time ($t_{1/2}$) of the supercoiled form (the time at which 50% of form I DNA is present) is 4.9 min, which indicates that the complex cleaves the DNA rapidly under these experimental conditions. We have also obtained the kinetic parameters $k_{obs2}$ and $t_{1/2}$ for the form II to form III conversion. The calculated values are $k_{obs2} = \sim 0.014\ min^{-1}$ ($R^2 = 0.96$) and $t_{1/2} = \sim 47.8$ min. As expected, the $k_{obs2}$ values obtained from this kinetic analysis are approximately 10 times lower than those of the corresponding $k_{obs1}$. In Hughes' work on

(72) Liu, J.; Zhang, T.; Qu, L.; Zhou, H.; Zhang, Q.; Liangian, J. *J. Inorg. Biochem.* **2002**, *91*, 269−276.
(73) Tu, C.; Shao, Y.; Gan, N.; Xu, Q.; Guo, Z. *Inorg. Chem.* **2004**, *43*, 4761−4766.
(74) Detmer, C. A., III; Pamatong, F. V.; Bocarsly, J. *Inorg. Chem.* **1996**, *35*, 6292−6298.
(75) Detmer, C. A., III; Pamatong, F. V.; Bocarsly, J. *Inorg. Chem.* **1997**, *36*, 3676−3682.
(76) González-Álvarez, M.; Alzuet, G.; Borrás, J.; Macías, B.; del Olmo, M.; Liu-González, M.; Sanz, F. *J. Inorg. Biochem.* **2002**, *89*, 29−35.
(77) Houk, B. E.; Hochhaus, G.; Hughes, J. A. *AAPS Pharmsci.* **1999**, *1* (4), 1−6.

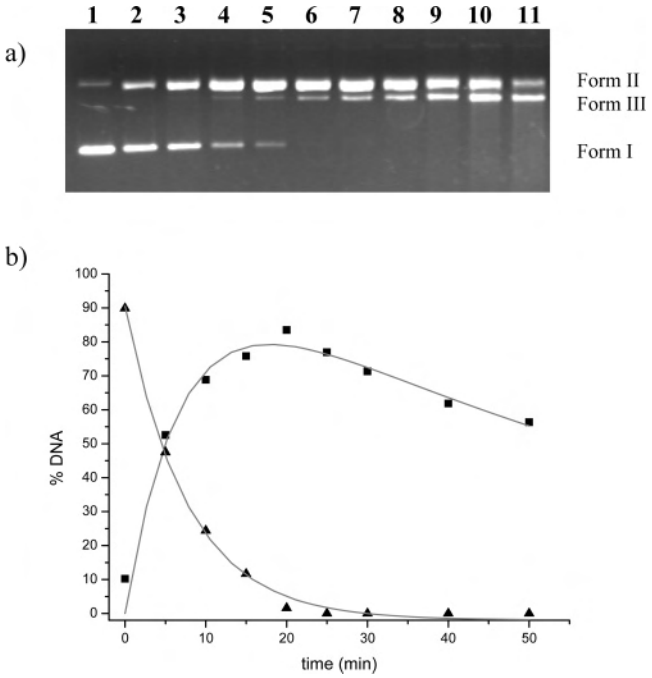


**Figure 9.** Cleavage activity of [Cu($\mu$-ade)(tol$SO_3$)(phen)]$_2$·2$H_2O$ monitored by 0.8% agarose gel electrophoresis, where [DNA] = 37.5 $\mu$M (in bp), [complex] = 9 $\mu$M, and [ascorbate] = 22.5 $\mu$M. (a) Gel image showing the three forms of DNA. Lane 1, supercoiled DNA; Lane 2, DNA + ascorbate (22.5 $\mu$M) (60 min); Lane 3, 5 min; Lane 4, 10 min; Lane 5, 15 min; Lane 6, 20 min; Lane 7, 25 min; Lane 8, 30 min; Lane 9, 40 min; Lane 10, 50 min; Lane 11, 60 min. (b) Experimental points and fitting curve for supercoiled DNA (▲) and circular relaxed DNA forms (■).

the degradation of plasmid DNA in rat plasma by natural nucleases,[77] the values for $k_{obs1}$ and $k_{obs2}$ were found to be 0.6 and 0.03 $min^{-1}$, respectively. These previously obtained $k_{obs}$ values are thus quite similar to those found for our compound under our assay conditions.

Previous studies have considered that an oxidative process for the form I to form II conversion follows a second-order profile.[78,79] Taking this as a precedent, we have established the following rate law:

$$\frac{\partial[\mathrm{DNA_I}]}{\partial t} = -k[\mathrm{complex}][\mathrm{DNA_I}]$$

where [$DNA_I$] represents the portion of supercoiled DNA, $t$ is the time, and $k$ is the second-order kinetic constant. From this equation, we obtain a value for $k = \sim 1.57 \times 10^4$ $M^{-1}$ $min^{-1}$. The higher value for this kinetic constant as compared to those for other copper complexes in oxidative cleavage with ascorbate[78] could be a consequence of both a synergistic effect between the two copper ions in the complex and an optimal complex interaction with the DNA. From the viscosity measurements, we had originally proposed an interaction either in the DNA grooves or with the sugar−phosphate backbone. The high value of the second-order constant $k$ suggests a proper orientation of the complex in the DNA grooves, usually close to C-4′H.

**Investigation of the DNA Cleavage Mechanism.** The implication of ROS (hydroxyl, superoxide, singlet oxygen-like species, hydrogen peroxide) in the nuclease mechanism can be inferred by monitoring the quenching of the DNA cleavage in the presence of ROS scavengers in solution. To clarify other aspects of the mechanism, the copper(I) chelator (neocuproine) and groove binders such as distamycin (minor-groove binder) or methyl green (major-groove binder) can also be used. Our results with these compounds are shown in Figure 10.

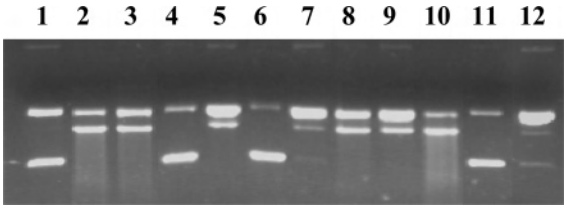


**Figure 10.** Agarose gel electrophoresis of pUC18 plasmid DNA treated with complex 9 $\mu$M and 22.5 $\mu$M of ascorbate. Incubation time 1 h (37 °C). Lane 1, supercoiled DNA control; Lane 2, DNA + complex without inhibitors; Lane 3, complex + 2,2,6,6-tetramethyl-4-piperidone; Lane 4, complex + Tiron; Lane 5, complex + sodium formate; Lane 6, complex + potassium iodide; Lane 7, complex + DMSO; Lane 8, complex + urea; Lane 9, complex + neocuproine; Lane 10, complex + methyl green; Lane 11, complex + catalase; Lane 12, complex + distamycin.

The addition of 2,2,6,6-tetramethyl-4-piperidone (lane 3) scarcely protects against the DNA strand breakage induced by the compound, which suggests that neither $^1O_2$ nor any other singlet oxygen-like entity participates in the oxidative cleavage. Lane 4 shows a significant reduction of DNA cleavage in the presence of Tiron, which indicates that $O_2^{\bullet -}$ is one of the reactive species required for the breakdown of DNA in this case. The addition of hydroxyl radical scavengers such as sodium formate, potassium iodide, DMSO, or urea (lanes 5, 6, 7, and 8, respectively) also attenuates the DNA strand scission mediated by the complex. These results suggest that hydroxyl radicals may be the reactive species involved in the cleavage process. The presence of neocuproine also diminishes the degradation of DNA. This attenuation of the cleavage activity can be explained by taking into consideration the reduction of the Cu(II) ion in the ROS production process. As for the catalase enzyme, it blocks the breakdown of the DNA (lane 11), indicating that hydrogen peroxide also participates in the cleavage process. In the presence of the major-groove binder methyl green, no apparent inhibition of DNA damage was observed, a finding that implies a lack of major binding preferences for the complex (lane 10). However, because the addition of distamycin produces a decrease in the cleavage capacity of the complex, a minor-groove interaction can be proposed, which is also in accordance with the conclusions drawn from the DNA binding and kinetic studies. The results were similar in MPA (data not shown).

On the basis of all of these results, we propose that the compound interacts with DNA through the minor groove, after which the copper(II) centers are reduced in the presence of an activating agent to copper(I) species. These subsequently react with dioxygen to give rise to the hydroxyl radicals (Chart 2) needed for DNA breakdown.

(78) Jin, Y.; Cowan, J. A. *J. Am. Chem. Soc.* **2005**, *127*, 8408−8415.

(79) Goodisman, J.; Kira, C.; Dabrowiak, J. C. *Biophys. Chem.* **1997**, *69*, 249−268.

**Chart 2**

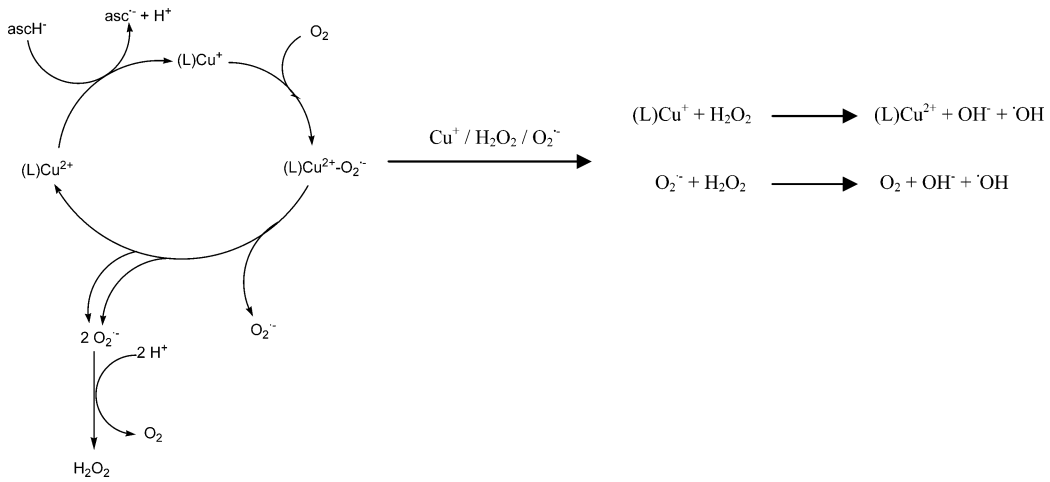


## Conclusions

The results reported here demonstrate that the dinuclear compound $[Cu(\mu\text{-ade})(tolSO_3)(phen)]_2 \cdot 2H_2O$ is very efficient in promoting the cleavage of plasmid DNA in the presence of different activators. Synergistic effects between the Cu(II) centers may contribute to its significant cleavage activity. The maximum rate of degradation of the supercoiled plasmid DNA form, obtained in the presence of 9 $\mu$M complex, is 0.141 $min^{-1}$, a value that corresponds to a half-life time of only 4.9 min. The results of the experiments aimed at defining the compound's mode of action point to a minor-groove interaction with the subsequent generation of active oxygen intermediates; these are then responsible for the actual DNA damage. Its high reactivity, due, at least in part, to the coordination of adenine and phenanthroline, makes the $[Cu(\mu\text{-ade})(tolSO_3)(phen)]_2 \cdot 2H_2O$ a very promising candidate for biological applications in vivo.

**Acknowledgment.** J.B., G.A., J.L.G.-G, and M.G.-A acknowledge financial support from the Spanish CICYT (grant CTQ2004-03735). A.C. thanks CICYT (grant CTQ-2006-15329-C02/BQU) for financial support.

**Supporting Information Available:** X-ray crystallographic files in CIF format. Crystal data and experimental details for *N*-9-(toluenesulfonyl)adenine (HL) and $[Cu(\mu\text{-ade})(tolSO_3)(phen)]_2 \cdot 2H_2O$ (Table S1). Interatomic distances and bond angles of *N*-9-(toluenesulfonyl)adenine (HL) (Table S2). *ORTEP* drawing of HL (Figure S1). Agarose gel electrophoresis of pUC18 plasmid DNA treated with the complex in the presence of 3-mercaptopropionic acid (MPA) (Figure S2). Agarose gel electrophoresis of pUC18 plasmid DNA treated with $[Cu(phen)_2]^{2+}$ in the presence of 3-mercaptopropionic acid (MPA) (Figure S3). This material is available free of charge via the Internet at http://pubs.acs.org.

IC700751J